33rd European Study Group with Industry
14 – 18 September 1998
pp. 27 – 35

Laser Drilling

F. van Beckum, J.B. van den Berg, S.J. Chapman,
P. Hemker, J. Jansen, R. Mattheij, T. Myers,
M. Peletier, F. Quirós, K. Verhoeven

Report prepared by S.J. Chapman and K. Verhoeven

1. Introduction

Since the first demonstrations of the ruby laser in 1960, the laser quickly took an important place in various domains of industry. This is mainly because of its concentrated and contactless energy supply. This has led to many applications in the domain of laser materials processing. The most important applications in this domain are cutting, welding and marking. Laser drilling, the topic of this article, is a niche application.

Laser percussion drilling (drilling by multiple shots) is for instance used in the process of gas turbine manufacturing, because of the fact that the components to be drilled are made of superalloys which are very hard to machine by conventional techniques. To fix ideas, the typical hole diameter, hole depth and pulse length are $0.5 \div 1.0$ mm, $3 \div 10$ mm and 1.0 ms, respectively. Laser percussion drilling is favoured over alternative drilling processes like spark erosion drilling and laser trepanning drilling because it is by far the fastest process. However, it suffers of problems with the quality of the hole. The main quality aspects are:

- Tapering (Decrease of hole diameter with depth)
- Recast layer (Re-solidified material at wall of hole)
- Bellow shape (Local increase of hole diameter)

The laser drilling process depends on the material properties and on the laser beam characteristics: wavelength and intensity as a function of space and time.

The main goal of the research being started at the study group is to come up with a simulation model based on a mathematical model which includes all relevant physical features. This model is needed to get a better understanding of the process and to be able to select proper settings of the process parameters. Once well validated, this model will be used to define the specification of the ideal laser used for drilling. The major problem will be to handle the different phases and in particular the modelling of the interaction of the beam with the vapour phase.

The setup of this article is as follows. Sections 2 to 4 are concerned with the phase transformations of the material irradiated. In Section 5 the fact that drilling velocities are found to be much higher than can be accounted for by vaporization only is explained by the so called piston mechanism. Then,

I	$15 \cdot 10^9$	W m^{-2}
ρ	$2.70 \cdot 10^3$	kg m^{-3}
L_v	$11723.040 \cdot 10^3$	J kg^{-1}
L_f	$355.878 \cdot 10^3$	J kg^{-1}
k	229.111	W m^{-1} K^{-1}
c	896	J kg^{-1} K^{-1}
T_m	931.15	K
T_v	2543.15	K
μ	$2.66 \cdot 10^{-3}$	Pa s

TABLE 1. Physical data for drilling Aluminium. (These data were taken from [4])

Section 6 gives a few ideas on how to model the interactions of the incoming laser beam with the vapour phase in front of the target. Finally, Section 7 gives some conclusions and recommendations.

2. Evaporation-controlled limit

The simplest case to consider is the situation in which all the energy supplied to the surface goes into vaporizing the material, as in [1]. This evaporation-controlled limit may arise either when the energy is applied to the surface too rapidly for the heat to be conducted into the material, or when the beam power density is constant and the temperature ahead of the evaporating boundary approaches a steady state. By equating the rate of input of energy to the rate of absorption of latent heat of vaporization, we find

$$I = v\rho L_v. \tag{1}$$

This gives the velocity of the vaporization boundary as

$$v = \frac{I}{\rho L_v}. \tag{2}$$

Table 1 lists the physical constants relevant to the problem for aluminium (a material for which they were readily available). Using these we find $v \approx 0.5$ ms^{-1}.

Drilling by pure evaporation is observed in sublimating materials or in metals at low irradiance. In experiments drilling velocities of more than 1 ms^{-1} are found. Thus, at higher irradiances, drilling velocities are found to be much higher (perhaps by factors of $2 \div 5$) than can be accounted for by evaporation alone. It is clear that some of the material must be ejected from the drilled hole in the liquid state, probably via the splashing mechanism that relies on the evaporation pressure (or recoil pressure), described by Von Allmen [2, 3]. Therefore, we now address the question of the size of the melt pool which forms during the pre-vaporization "warm up" phase.

3. The melting model

The temperatures in both the liquid and the solid region are governed by the heat equation. We concentrate on diffusion of heat in the direction of drilling,

neglecting radial diffusion. For typical drilling parameters, this is shown in [1] to be a reasonable approximation.

Thus we have the following one-dimensional model

$$k_i \frac{\partial^2 T_i}{\partial x^2} = \rho c_i \frac{\partial T_i}{\partial t} \quad \text{in } \Omega_i \qquad \text{for } i = s, l, \tag{3}$$

where k, ρ and c are the thermal conductivity, density and specific heat capacity respectively, and the subscripts s and l denote the solid and the liquid. Furthermore, Ω_l denotes the liquid region $0 \leq x < x_0(t)$ and Ω_s the solid region $x_0(t) < x < \infty$ where $x_0(t)$ is the position of the solid-liquid interface defined by $T(x_0(t), t) = T_m$. At the the boundary $x = 0$ the energy is supplied,

$$k_l \frac{\partial T_l}{\partial x} = -I \qquad \text{at } x = 0. \tag{4}$$

At the solid-liquid interface the so called Stefan condition and continuity of temperature hold, yielding

$$k_l \frac{\partial T_l}{\partial x} - k_s \frac{\partial T_s}{\partial x} = -v_n L_f \rho \qquad \text{at } x = x_0(t), \tag{5}$$

$$T = T_m. \tag{6}$$

Here, v_n is the velocity of the interface in normal direction, where the normal $\mathbf{n}$ is the normal pointing into the solid and furthermore, L_f is the latent heat of fusion. At infinity, the boundary condition

$$T_s \to T_0 \qquad \text{as } x \to \infty \tag{7}$$

holds, where T_0 is the ambient temperature of the material. We nondimensionalize this by introducing the dimensionless variables $\overline{x}$, $\overline{t}$ and $\overline{T}$, defined by

$$x = x^* \overline{x} \quad = \quad \frac{k(T_v - T_m)}{I} \overline{x}, \tag{8}$$

$$t = t^* \overline{t} \quad = \quad \frac{\rho c k (T_v - T_m)^2}{I^2} \overline{t}, \tag{9}$$

$$T \quad = \quad T_m + (T_v - T_m)\overline{T}, \tag{10}$$

where we have assumed that k and c take the same values in the solid and liquid phases. Using the material data for aluminium gives the length and time scales $x^* \approx 2.5 \cdot 10^{-5}$m and $t^* \approx 6.4 \cdot 10^{-6}$s. Writing the equations together with the boundary conditions in dimensionless form we obtain the Stefan problem

$$\begin{cases} \dfrac{\partial^2 \overline{T}}{\partial \overline{x}^2} = \dfrac{\partial \overline{T}}{\partial \overline{t}} & \text{in } \Omega_i \quad i = s, l, \\ \dfrac{\partial \overline{T}}{\partial \overline{x}} = -1 & \text{at } \overline{x} = 0, \\ \overline{T} = 0; \ \left[\dfrac{\partial \overline{T}}{\partial \overline{x}}\right] = -\overline{L}_f v_n & \text{at } \overline{x} = \overline{x}_0(t), \\ \overline{T} \to \overline{T}_0 & \text{as } \overline{x} \to \infty, \end{cases} \tag{11}$$

where $\overline{L}_f = \frac{L_f}{c(T_v - T_m)}$ is the dimensionless latent heat of fusion, $\overline{T}_0 = \frac{T_0 - T_m}{T_v - T_m}$, and $\overline{x}_0(t)$ is the dimensionless position of the solid/liquid interface. With the material properties of aluminium we find $\overline{L}_f \approx 0.25$ (in fact $\overline{L}_f$ is small in almost all metals). In this case as a first approximation we can neglect the discontinuity in the temperature gradient due to the solid-liquid phase transition. This leads to the following problem

$$\begin{cases} \dfrac{\partial^2 \overline{T}}{\partial \overline{x}^2} = \dfrac{\partial \overline{T}}{\partial \overline{t}} & \text{in } \overline{x} > 0, \\ \dfrac{\partial \overline{T}}{\partial \overline{x}} = -1 & \text{at } \overline{x} = 0, \\ \overline{T} \to \overline{T}_0 & \text{as } \overline{x} \to \infty. \end{cases} \tag{12}$$

with solution [1]

$$\overline{T}(\overline{x}, \overline{t}) = 2 \left(\frac{\overline{t}}{\pi} \right)^{\frac{1}{2}} \exp\left(-\frac{\overline{x}^2}{4\overline{t}} \right) - \overline{x} \operatorname{erfc}\left(\frac{\overline{x}}{2\overline{t}^{\frac{1}{2}}} \right) + \overline{T}_0. \tag{13}$$

To determine the time at which the surface starts to vaporize, we note that

$$\overline{T}(0, \overline{t}) = 2 \left(\frac{\overline{t}}{\pi} \right)^{\frac{1}{2}} + \overline{T}_0, \tag{14}$$

and that vaporization begins when $\overline{T}(0, \overline{t}) = 1$, i.e. $\overline{t} = (1 - \overline{T}_0)\pi/4$. The dimensionless melt pool depth is given by $\overline{x}_0(t)$, defined by $\overline{T}(\overline{x}_0(t), \overline{t}) = 0$, giving

$$2 \left(\frac{\overline{t}}{\pi} \right)^{\frac{1}{2}} \exp\left(-\frac{\overline{x}_0^2}{4\overline{t}} \right) - \overline{x}_0 \operatorname{erfc}\left(\frac{\overline{x}_0}{2\overline{t}^{\frac{1}{2}}} \right) = -\overline{T}_0. \tag{15}$$

However, from the small length and time scales it follows that vaporization takes place very quickly and the melt pool is very small as vaporization starts. Hence if the melt pool splashes out as soon as vaporization begins it must do so many times per laser pulse, with a tiny amount of melt ejected each time.

Let us now consider the contrasting situation in which there is no immediate splash, to determine the maximum possible size of the melt pool ahead of the evaporating boundary.

4. Evaporation and melting

Once the material starts to vaporize the (dimensionless) Stefan problem (11) needs to be modified to include a Stefan condition and temperature condition at the vaporizing boundary. In dimensionless form these are given by

$$\frac{\partial \overline{T}}{\partial \overline{x}} = -1 + \frac{v_v}{\varepsilon}; \quad \overline{T} = 1. \tag{16}$$

where, $\varepsilon = \frac{c(T_v - T_m)}{L_v}$ measures the ratio of the thermal energy required to heat the material from its melting point to its vaporization point to the latent heat of vaporization. In the case of aluminium we have $\varepsilon \approx 0.12$, and ε is small for most metals. Hence it is sensible to consider the limit of small ε. However, a rescaling is necessary, since the boundary condition implies that the vaporizing boundary is stationary on the present length-scales and time-scales. Thus we introduce $\tilde{x}$ and $\tilde{t}$ by defining

$$\overline{x} = \frac{\tilde{x}}{\varepsilon}, \qquad \overline{t} = \frac{\tilde{t}}{\varepsilon^2}. \tag{17}$$

The new length and time scales are then $x^*/\varepsilon \approx 10^{-4}$m and $t^*/\varepsilon^2 \approx 1.5 \cdot 10^{-4}$s. We now have

$$\begin{cases} \dfrac{\partial^2 \overline{T}}{\partial \tilde{x}^2} = \dfrac{\partial \overline{T}}{\partial \tilde{t}}, & \text{in } \Omega_i, \quad i = s, l, \\ \overline{T} = 1; \quad \varepsilon \dfrac{\partial \overline{T}}{\partial \tilde{x}} = -1 + v_v, & \text{at } x = \tilde{x}_1(t), \\ \overline{T} = 0; \quad \dfrac{\partial \overline{T}}{\partial \tilde{x}} = -\overline{L}_f v_l, & \text{at } x = \tilde{x}_0(t), \\ \overline{T} \to \overline{T}_0 & \text{as } \tilde{x} \to \infty, \end{cases} \tag{18}$$

where $\tilde{x}_1(t)$ is the dimensionless position of the vaporizing boundary. The previous (pre-vaporization) problem corresponds to the small time behaviour of this problem. As $\overline{L}_f \to 0$, $\varepsilon \to 0$ the leading order problem is given by

$$\begin{cases} \dfrac{\partial^2 \overline{T}}{\partial \tilde{x}} = \dfrac{\partial \overline{T}}{\partial \tilde{t}} & \text{in material,} \\ \overline{T} = 1; \quad 0 = -1 + v_v & \text{at the vaporizing boundary.} \end{cases} \tag{19}$$

Hence $v_v = 1$ to leading order. This is exactly the evaporation limited solution that we found previously, and gives the dimensional speed of the vaporization boundary as $v_v \approx 0.7$ ms^{-1}. The solution for $\overline{T}$ is [1]

$$\overline{T}(\tilde{x}, \tilde{t}) = \left(\frac{1}{2} e^{-(\tilde{x} - \tilde{t})} \operatorname{erfc} \left(\frac{\left(\frac{1}{2}\tilde{x} - \tilde{t}\right)}{\tilde{t}^{\frac{1}{2}}} \right) + \frac{1}{2} \operatorname{erfc} \left(\frac{\tilde{x}}{2\tilde{t}^{\frac{1}{2}}} \right) \right) (1 - \overline{T}_0) + \overline{T}_0 . \tag{20}$$

The position of the melt pool boundary $\tilde{x}_0(\tilde{t})$ is again given by $\overline{T}(\tilde{x}_0(\tilde{t}), \tilde{t}) = 0$, giving

$$\frac{1}{2} e^{-(\tilde{x}_0 - \tilde{t})} \operatorname{erfc} \left(\frac{\left(\frac{\tilde{x}_0}{2} - \tilde{t}\right)}{\tilde{t}^{\frac{1}{2}}} \right) + \frac{1}{2} \operatorname{erfc} \left(\frac{\tilde{x}_0}{2\tilde{t}^{\frac{1}{2}}} \right) = -\frac{\overline{T}_0}{1 - \overline{T}_0}. \tag{21}$$

For large times we find

$$\tilde{x}_0(\tilde{t}) \sim \tilde{t} + \log \left(\frac{1 - \overline{T}_0}{\overline{T}_0} \right). \tag{22}$$

Since $\tilde{x}_1 = \tilde{t}$, it follows that the size of the melt pool $\tilde{x}_0 - \tilde{x}_1$ approaches (from below) the constant value

$$\log\left(\frac{1-\overline{T}_0}{\overline{T}_0}\right)$$

as the vapourization proceeds. This gives the maximum size of the melt pool available for ejection through splashing.

5. The piston mechanism

As we have already noted, at high irradiances drilling velocities in metals are often found to be much higher than can be accounted for by evaporation only. The reason is that much of the metal extracted leaves the hole as melt rather than as vapour. One mode of melt ejection is the piston mechanism as illustrated in Figure 1, in which the melt is squirted out of the hole by the recoil pressure at the evaporating boundary. We could now ask ourselves the question

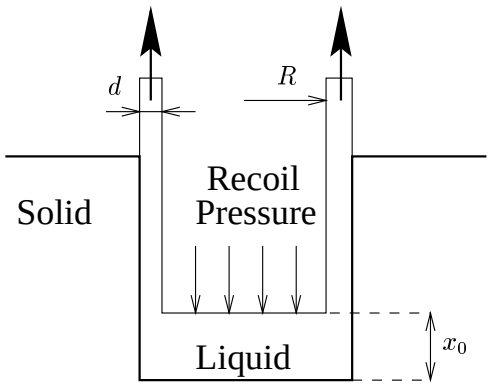

Figure 1. The piston mechanism.

as to how quickly does the fluid get expelled by the recoil pressure.

We obtain this velocity by balancing the forces. The work done by the recoil pressure, assuming that the total amount of liquid drawn in Figure 1 is squirted out, is

$$p\pi R^2 x_0. \tag{23}$$

If the fluid is expelled quickly (which can be verified a posteriori) the flow will be high Reynolds number, and we can neglect viscous dissipation. Then this energy will all be converted to kinetic energy, i.e.

$$\left(\frac{1}{2}\rho u^2\right) \times \pi R^2 x_0. \tag{24}$$

This gives the velocity,

$$u = \left(\frac{2p}{\rho}\right)^{\frac{1}{2}}. \tag{25}$$

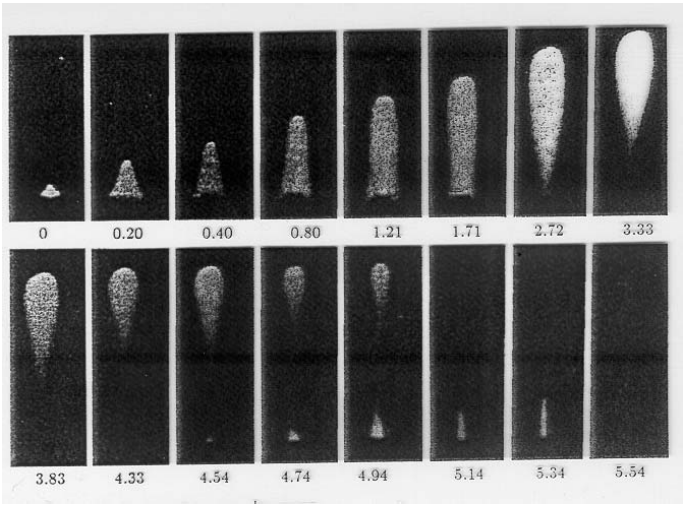

FIGURE 2. High-speed camera frames of a vapour cloud from an aluminium alloy irradiated by 5 ms, 1.5MW/cm^2 CO_2-laser pulses (incident from above). Blocking of the incoming radiation by the plume can be seen. Numbers below the frames give the time in ms.

VON ALLMEN [3] gives an example in which a speed up to 50 ms^{-1} is reached. Assuming this speed in the case of aluminium would give a Reynolds number of

$$\mathrm{Re} = \frac{\rho u L}{\mu} \approx 5 \cdot 10^4, \tag{26}$$

where L is the characteristic length (1 mm). This supports the assumption of neglecting viscous dissipation.

6. THE VAPOUR MODEL

In the previous sections one of the assumptions used to derive the models was the transparency of the vapour. In many cases, especially considering irradiations in the intensity regime used to drill, this assumption is not valid, as can be seen in Figure 2. In this figure it is easy to see that the vapour plume absorbs the incoming radiation by noting that this plume shields the target completely (frames 8 to 10). Therefore a model has to be made that also takes into account the absorption of incoming energy by the vapour plume in front of the target. Possible first steps towards such a model are presented in this section. Section 6.1 takes this step by using conservation of both mass and momentum, whereas section 6.2 uses the so called Rankine-Hugoniot approach, that is, one models the vapour as a shock wave.

6.1. Balance Equations

First we try to model the vapour in one dimension where we define $x = 0$ to be the top of the hole and $x = h$ to be the depth of the hole. Conservation of mass and of momentum give us

$$\frac{\partial \rho}{\partial t} + \frac{\partial}{\partial x}(\rho u) = 0, \tag{27}$$

$$\frac{\partial}{\partial t}(\rho u) + \frac{\partial}{\partial x}(\rho u^2) + \frac{\partial p}{\partial x} = 0, \tag{28}$$

respectively. Here, u is the speed of the vapour ρ is its density and p is the pressure. Furthermore we assume the mass-flux ρu to be given at $x = h$, and the density ρ and the pressure p to be the ambient density ρ_0 and ambient pressure p_0 at $x = 0$, respectively.

If we assume the vapour to be an ideal gass, a rather crude assumption, we are able to solve this system numerically.

This model has to be extended by including an equation that models the absorption of radiation by the vapour and by an equation that models the temperature rise of the vapour as a function of the absorbed intensity. With this model we can compute the amount of energy that reaches the bottom of the hole, and therefore can be used to determine the time at which the target is shielded by the vapour.

6.2. The Rankine-Hugoniot Approach

Another approach to model the vapour makes use of the idea that the front of the vapour plume can be modelled as a density shock wave. Denote the conditions in front of the shock wave by the subscript $-$ and the conditions after the shock wave by the subscript $+$. Using the assumption that the vapour can be modelled as an ideal gass, the so-called Rankine-Hugoniot relations are given by

$$[\rho]\dot{s} + [\rho u] = 0, \tag{29}$$

$$[\rho u]\dot{s} + [\rho u^2 + RT\rho] = 0. \tag{30}$$

Here, $x = s(t)$ denotes the position of the shock, and $[\,\cdot\,]$ denotes the jump across the shock. This leads to

$$\frac{[\rho u]}{[\rho]} = \frac{[\rho u^2 + RT\rho]}{[\rho u]}. \tag{31}$$

Assuming $u_- = 0$ leads to

$$\rho_+(\rho_+ - \rho_-)^2 = \frac{\rho_-(\rho_+ u_+)^2}{RT}. \tag{32}$$

Knowing the mass flux $\rho_+ u_+$ and ρ_- this equation fixes ρ_+ and thereby u_+. Now we can compute the speed of the shock wave by

$$\dot{s} = -\frac{[\rho u]}{[\rho]}. \tag{33}$$

7. Conclusions and Remarks

We have examined various aspects of the laser drilling process. We first examined the simplest case of the evaporating-controlled limit, in which all the energy supplied by the laser is used in vaporizing the material. This predicts drilling velocities lower than those observed in experiments, which leads to the conclusion that some of the material removed from the hole must be ejected in a liquid state rather than in a vapour state.

We therefore turned our attention to the size of the melt pool which is formed during the drilling process. We found that in the "warm up" stage before vaporization begins the melt pool formed is very small, so that if it is splashed out immediately the surface starts to vaporize there must be a high frequency of very small splashes.

We then considered the case in which the melt is not splashed out immediately, but remains for a while as vaporization is taking place. We found that the melt pool increases in size considerably up to a maximum value which is easily calculated. However, during this vaporization phase most of the energy supplied to the surface of the irradiated material goes into vaporization, with only a small amount being used to create the melt pool.

Since it is more efficient to splash out melt than to vaporize it, improved control of the melt pool may lead to more efficient drilling. One possibility is to try to generate a large melt pool with a minimum of evaporation by applying a relative low intensity pulse, followed by a high intensity pulse to generate high evaporation producing the recoil pressure to splash out this melt pool. This may also help to minimize the recast layer formed by the collapse of the final splash when the hole breaks through the material, since the melted region will break through before the final splash and the final melt will be ejected through the hole rather than back.

Although the studygroup came to some results for the process of absorption of energy in the vapour plume in front of the target, and the two different approaches to tackle the absorption presented in this article are promising, this topic needs further research and a more sophisticated modelling. Furthermore, experimental results have to be obtained to validate the vaporization models.

References

1. J.G. Andrews & D.R. Atthey, *On the motion of an intensely heated evaporating boundary.* J. Inst. Maths. Applics. **15**, 59–72 (1975).
2. M. von Allmen, *Laser drilling velocity in metals*, Journal of Applied Physics, **47**, no. 12, pp. 5460–5463 (1976).
3. M. von Allmen & A. Blatter, *Laser-beam interactions with materials*, Springer-Verlag, Berlin, (1995).
4. K. Ražnjević, *Handbook of thermodynamic tables and charts*, McGraw-Hill, New York, (1976).